Supplementary Information

Crystalline boron monosulfide nanosheets with tunable bandgaps

Haruki Kusaka,†[a] Ryota Ishibiki,†[a] Masayuki Toyoda,†[b] Takeshi Fujita,[c] Tomoharu Tokunaga,[d] Akiyasu Yamamoto,[ef] Masashi Miyakawa,[g] Kyosuke Matsushita,[h] Keisuke Miyazaki,[i] Linghui Li,[a] Satish Laxman Shinde,[j] Mariana S. L. Lima,[a] Takeaki Sakurai,[kl] Eiji Nishibori,[lm] Takuya Masuda,[h] Koji Horiba[n], Kenji Watanabe,[g] Susumu Saito,[bfo] Masahiro Miyauchi,[i] Takashi Taniguchi,[p] Hideo Hosono[fp] and Takahiro Kondo*[fjl]

[a]*Graduate School of Pure and Applied Sciences, University of Tsukuba, Tsukuba 305-8573, Japan*
[b]*Department of Physics, Tokyo Institute of Technology, Meguro-ku, Tokyo 152-8551, Japan*
[c]*School of Environmental Science and Engineering, Kochi University of Technology, Kochi 782-8502, Japan*
[d]*Graduate School of Engineering Materials Design Innovation Engineering, Nagoya University, Aichi 464-8601, Japan*
[e]*Institute of Engineering, Tokyo University of Agriculture and Technology, Tokyo 183-8538, Japan*
[f]*Materials Research Centre for Element Strategy, Tokyo Institute of Technology, Yokohama 226-8503, Japan*
[g]*Research Center for Functional Materials, National Institute for Materials Science, Tsukuba 305-0044, Japan*
[h]*Center for Green Research on Energy and Environmental Materials, National Institute for Materials Science, Tsukuba 305-0044, Japan*
[i]*Department of Materials Science and Engineering, School of Materials and Chemical Technology, Tokyo Institute of Technology, Meguro-ku, Tokyo 152-8552, Japan*
[j]*Department of Materials Science, Faculty of Pure and Applied Sciences, University of Tsukuba, Tsukuba 305-8573, Japan*
[k]*Department of Applied Science, Faculty of Pure and Applied Sciences, University of Tsukuba, Tsukuba 305-8573, Japan*
[l]*Tsukuba Research Center for Energy Materials Science, Faculty of Pure and Applied Sciences, University of Tsukuba, Tsukuba 305-8573, Japan*
[m]*Department of Physics, Faculty of Pure and Applied Sciences, University of Tsukuba, Tsukuba 305-8571, Japan*
[n]*Condensed Matter Research Center and Photon Factory, Institute of Materials Structure Science, High Energy Accelerator Research Organization (KEK), Tsukuba 305-0801, Japan*
[o]*Advanced Research Center for Quantum Physics and Nanoscience, Tokyo Institute of Technology, Meguro-ku, Tokyo 152-8551, Japan*
[p]*International Center for Materials Nanoarchitectonics, National Institute for Materials Science, Tsukuba 305-0044, Japan*

†These authors contributed equally
*Correspondence to: takahiro@ims.tsukuba.ac.jp

This file includes:

Table S1. Crystal data for rhombohedral boron monosulfide (r-BS) derived by Rietveld analysis.

Crystal data					
Crystal system, space group	Trigonal, $R\bar{3}m$				
Temperature (K)	300				
a, c (Å)	3.05070, 20.3846 (1)				
V (Å^3)	164.30 (1)				
Z	3				
Radiation type	Synchrotron, λ = 1.07900 Å				
Selected bond lengths (Å) B—B	1.6756 (1)				
Fractional atomic coordinates (x, y, z (Å)) and isotropic or equivalent isotropic displacement parameters (U_{iso} (Å^2))		x	y	z	U_{iso}
	S	0.00000	0.00000	0.54110(8)	0.0055(5)
	B	0.00000	0.00000	0.24969(3)	0.0055(5)

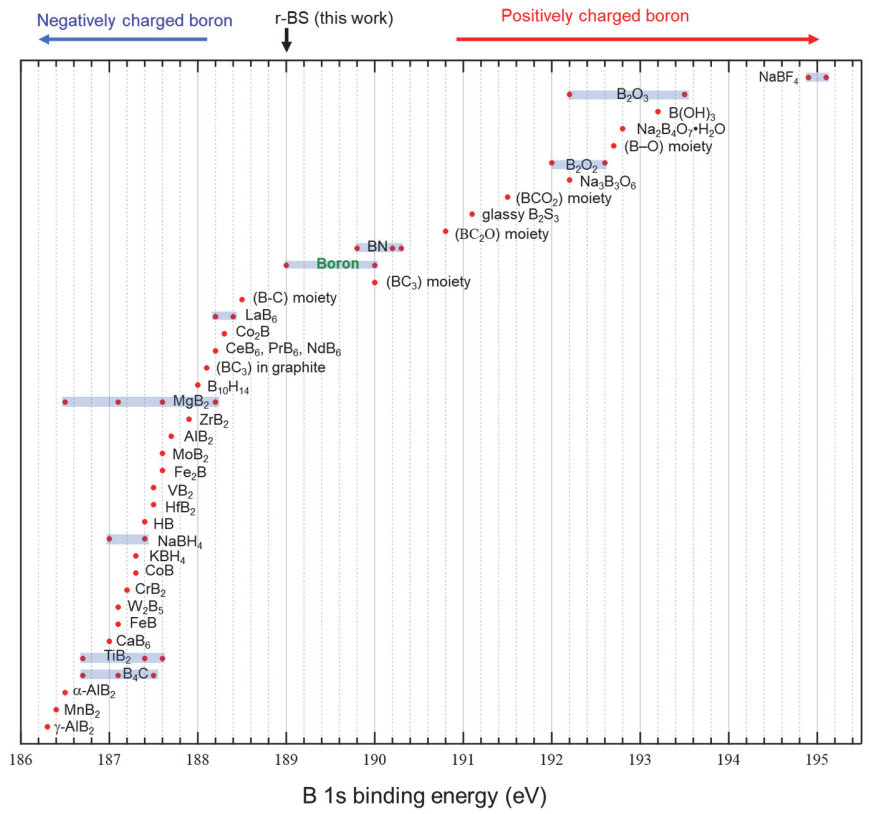

BE (eV)	Species	Reference
202.8	BF_3(vapor)	[1]
199.8	BCl_3(vapor)	[1]
199.0	BBr_3(vapor)	[1]
197.8	BI_3(vapor)	[1]
196.5	B_2H_6(vapor)	[1]
194.9-195.1	$NaBF_4$	[2,3]
192.2-193.5	B_2O_3	[3,4]
193.2	$B(OH)_3$	[2]
192.8	$Na_2B_4O_7 \cdot H_2O$	[2]
192.7	(B–O) moiety	[5,6]
192.0-192.6	B_2O_2	[3,7]
192.2	$Na_3B_3O_6$	[2]
191.5	(BCO_2) moiety	[5]
191.1	glassy B_2S_3	[37]
190.8	(BC_2O) moiety	[5]
190.0	(BC_3) moiety	[6]
189.0-190.0	boron	[3]
189.8-190.3	BN	[2,3]
188.5	(B–C) moiety	[8]
188.2-188.4	LaB_6	[7, 9,10]
188.3	Co_2B	[11]
188.2	CeB_6, PrB_6, NdB_6	[10]
188.1	(BC_3) in graphite	[12]
188.0	$B_{10}H_{14}$	[2]
187.9	ZrB_2	[13]
187.7	AlB_2	[11]
187.6	MoB_2	[11]
187.6	Fe_2B	[11]
187.5	VB_2	[11]
187.5	HfB_2	[11]
187.4	HB	[14]
187.0-187.4	$NaBH_4$	[1,3]
187.3	KBH_4	[38]
187.3	CoB	[11]
187.2	CrB_2	[11]
187.1	W_2B_5	[11]
187.1	FeB	[11]
187.0	CaB_6	[15]
186.7	TiB_2	[11,33-35]
186.5-188.2	MgB_2	[16-18,36]
186.7-187.5	B_4C	[2,8,12]
186.5	α-AlB_2	[11]
186.4	MnB_2	[11]
186.3	γ-AlB_2	[11]

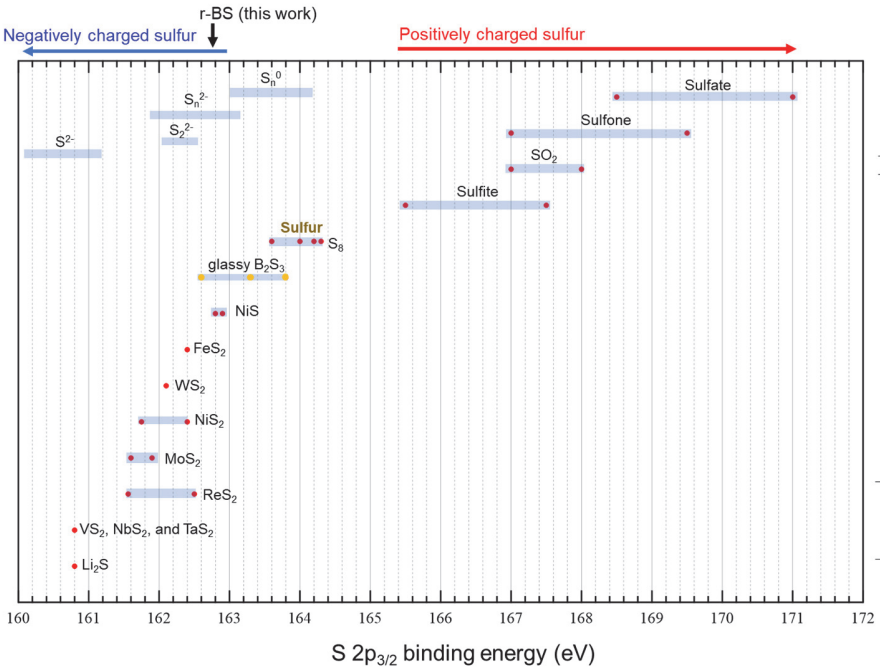

BE (eV)	Species	Reference
174.5-177.0	SF_6	[3]
168.5-171.0	Sulfate	[3,19]
167.0-169.5	Sulfone	[3,19]
167.0-168.0	SO_2	[3,19]
165.5-167.5	Sulfite	[3,19]
163.6-164.3	S_8	[3,19-21]
162.6, 163.3, 163.8	glassy B_2S_3	[37]
162.8-162.9	NiS	[22]
162.4	FeS_2	[23]
162.1	WS_2	[24]
161.75-162.4	NiS_2	[25,26]
161.6-161.9	MoS_2	[27,28]
161.56-162.5	ReS_2	[29,30]
160.8	VS_2, NbS_2, and TaS_2	[31]
160.8	Li_2S	[32]
160.1-161.2	S^{2-}	[20]
162.1-162.6	S_2^{2-}	[20]
161.9-163.2	S_n^{2-}	[20]
163.0-164.2	S_n^0	[20]

Figure S1. B 1s and S 2p binding energies for several compounds reported in the literature.

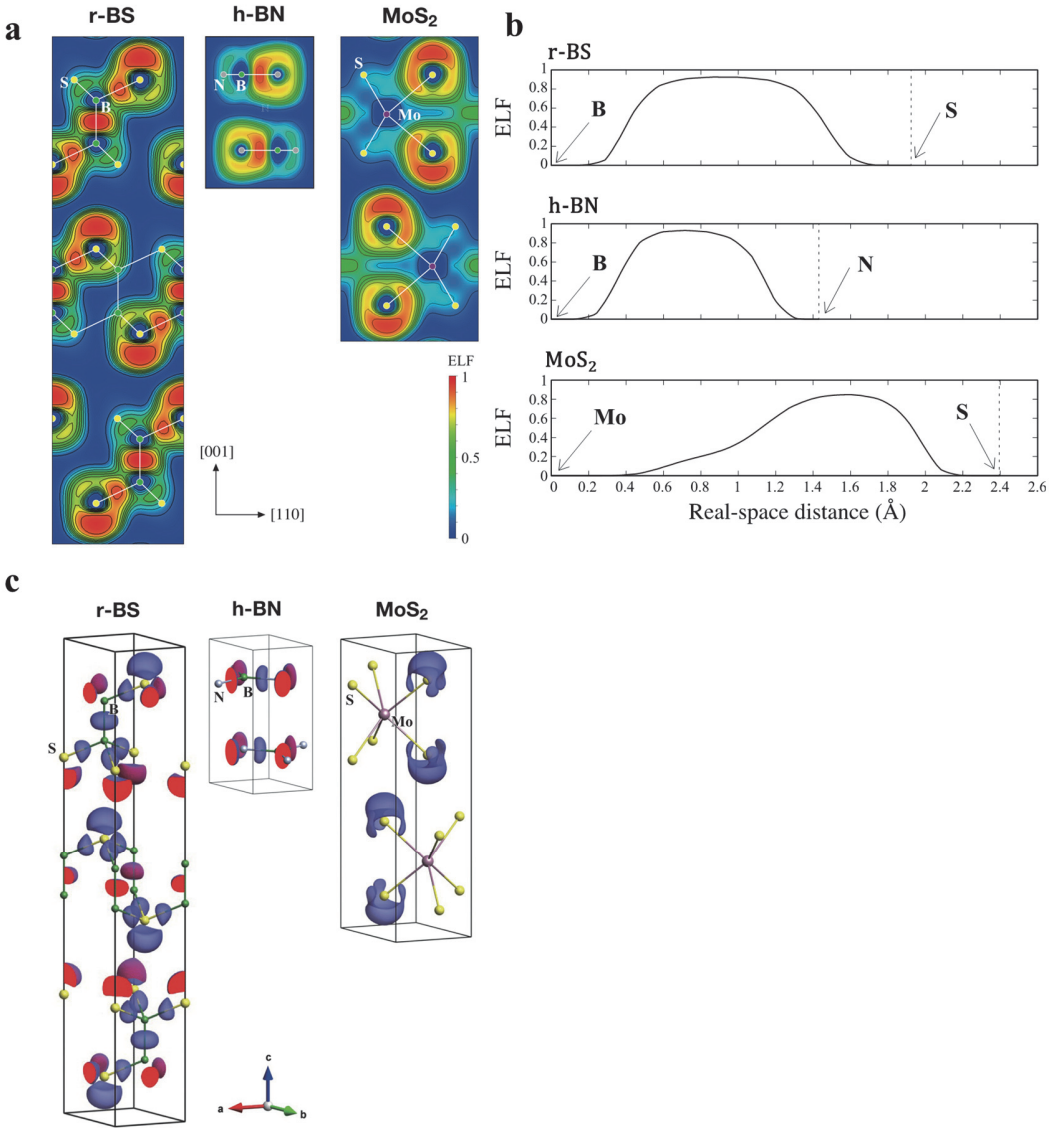

Figure S2 Calculated electron localization functions (EFLs) of r-BS, boron nitride (BN), and molybdenum disulfide (MoS_2). **a** Cross-sectional ELF images along the (110) plane for r-BS, h-BN, and MoS_2. **b** ELF profiles along the chemical bonds in r-BS, h-BN, and MoS_2. Both r-BS and h-BN show ELF maxima at midpoints between the respective atoms indicative of the formation of covalent bonds, while maximum intensity is observed near the sulfur in MoS_2, consistent with ionic bonding. **c** Three-dimensional ELF surfaces (at isosurfaces values of 0.85) for r-BS, h-BN, and MoS_2. The slightly larger surface contributions of the top and bottom regions of each BS layer are due to the accumulation of charge in the p_z orbitals of sulfur, which explains the slightly negatively charged sulfur suggested by S $2p_{3/2}$ peak position (Fig. 1b).

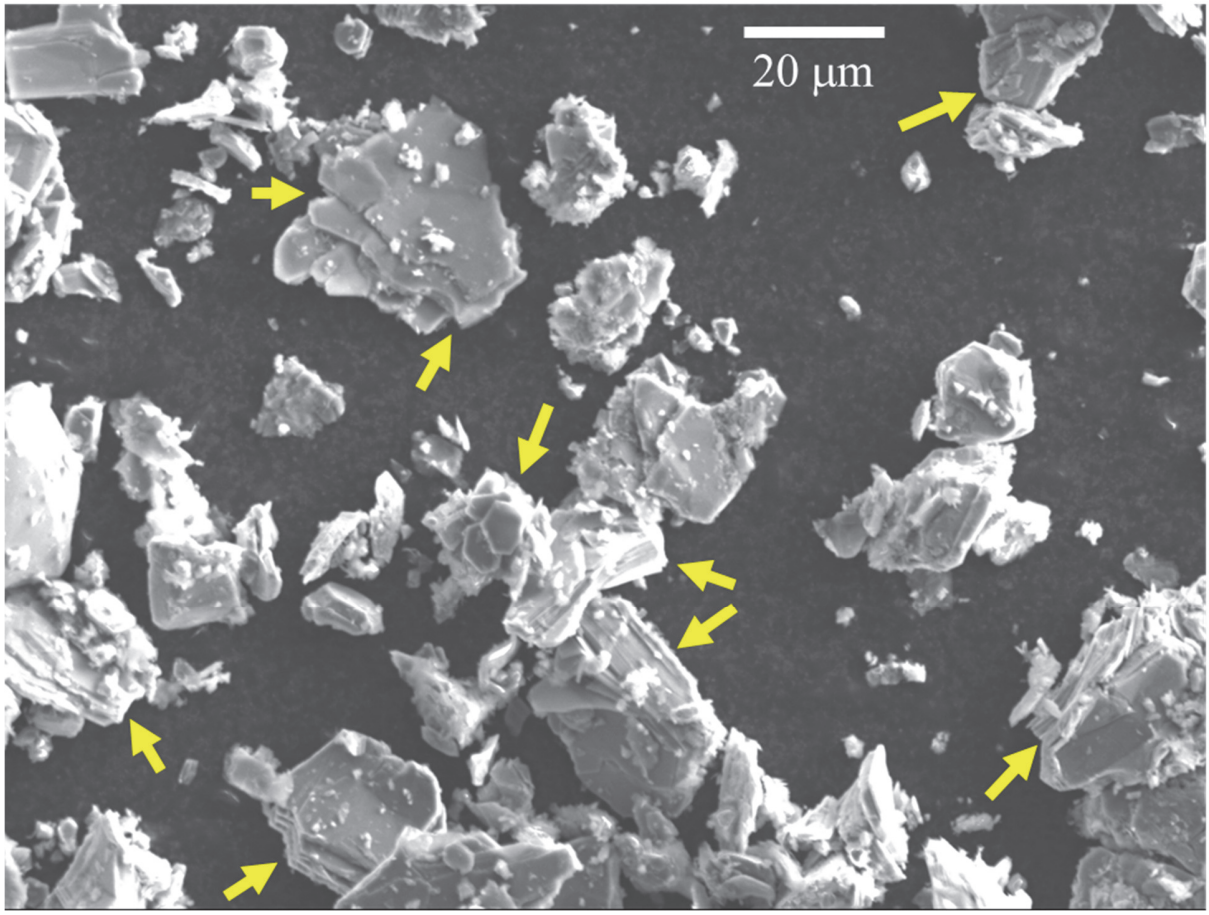

Figure S3. Scanning electron microscopy (SEM) image of r-BS particles on a Si surface. Incident energy of electron beam: 10 kV. Stacked layers can be seen in the image, as indicated by yellow arrows.

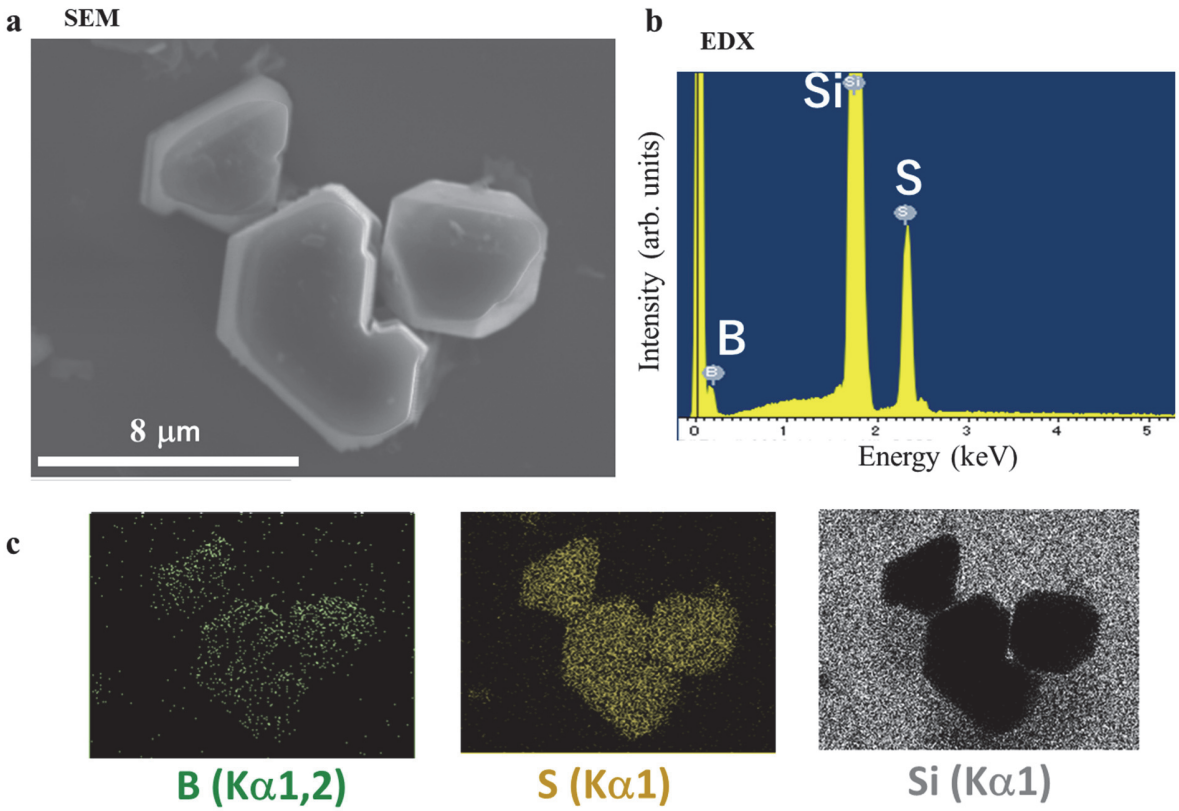

Figure S4. SEM and energy dispersive X-ray spectroscopy (EDX) data for r-BS on a Si surface. **a** SEM image of r-BS on Si surface. **b** EDX of r-BS on Si surface. **c** Elemental maps of r-BS (here, the B: $K_{\alpha 1}$,2, S: $K_{\alpha 1}$, and Si: $K_{\alpha 1}$ intensities are shown in green, yellow, and white, respectively).

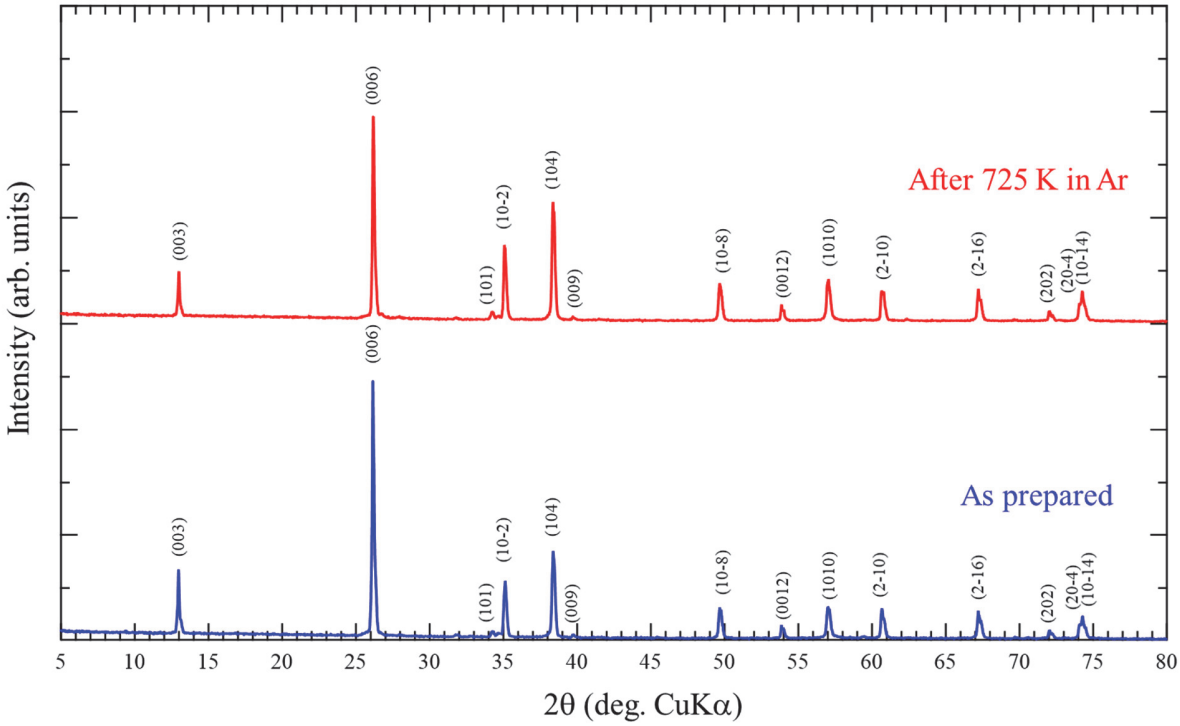

Figure S5. X-ray diffraction (XRD) patterns of r-BS powder before (as prepared) and heating at 725 K in a flow of Ar for 30 min.

Table S2. Calculated effective mass of r-BS and monolayer BS using DFT-LDA. The eigenvalues of the effective mass tensor (m_1, m_2, and m_3), as well as the harmonic averaged mass m^*, are shown in units of electron mass (m_e) or hole mass (m_h).

		m_1	m_2	m_3	m^*
Bulk r-BS	*elec.*	2.20	0.56	0.20	0.41
	hole	2.04	2.04	0.23	0.57
Monolayer BS	*elec.*	2.27	0.16	–	0.29
	hole	15.60	4.47	–	6.95

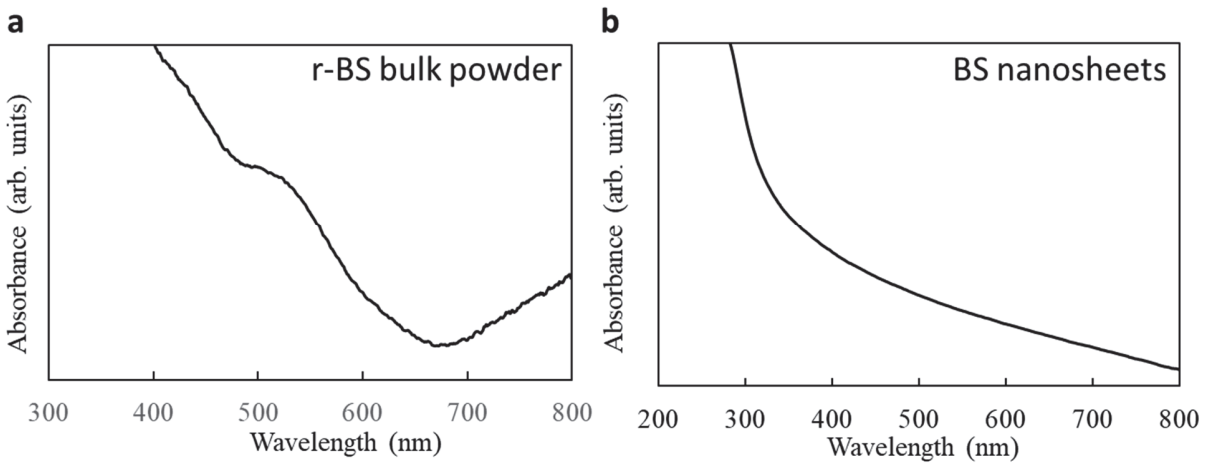

Figure S6. Ultraviolet-Visible (UV-Vis) absorption spectra for r-BS bulk powder and r-BS nanosheets. a. UV-Vis absorption spectrum of r-BS bulk powder recorded by the diffuse reflectance method using an integration sphere unit. b. UV-Vis absorption spectrum of the BS nanosheets dispersed in acetonitrile measured under transmittance mode using a quartz cell.

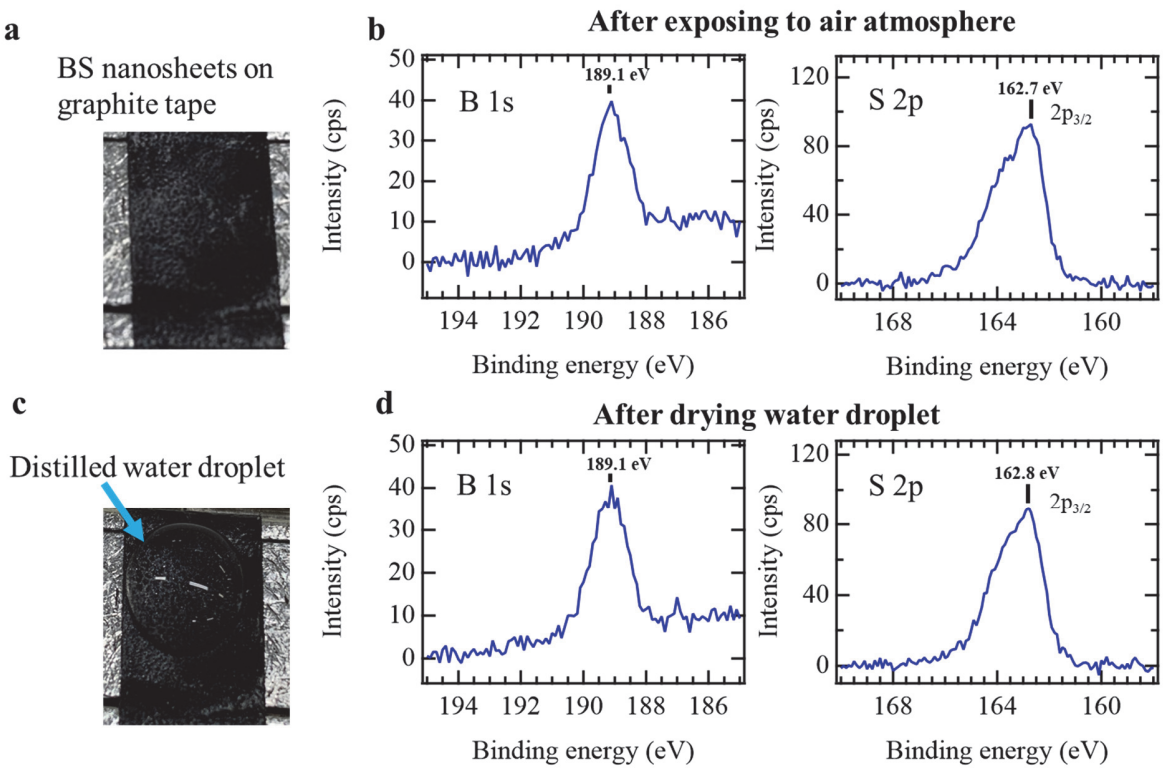

Figure S7. Environmental stability of BS nanosheets. **a.** Image of the BS nanosheets prepared using the Scotch-tape method on graphite tape. **b.** XPS profiles of BS nanosheets after exposure to air (the sample is the same as the one shown in panel a). Similar to Fig. 1b, the XPS profile does not show any additional oxide peak, indicating that the BS nanosheets are stable in air. **c** Image of the distilled water droplet on BS nanosheets prepared using the Scotch-tape method on graphite tape. **d** XPS profiles of BS nanosheets after drying the water droplet by evacuating in vacuum for 10 h (the sample is the same as the sample shown in panel c). Similar to Fig. 1b, the XPS profile does not show any additional oxide peak, indicating that the BS nanosheets are stable against water.

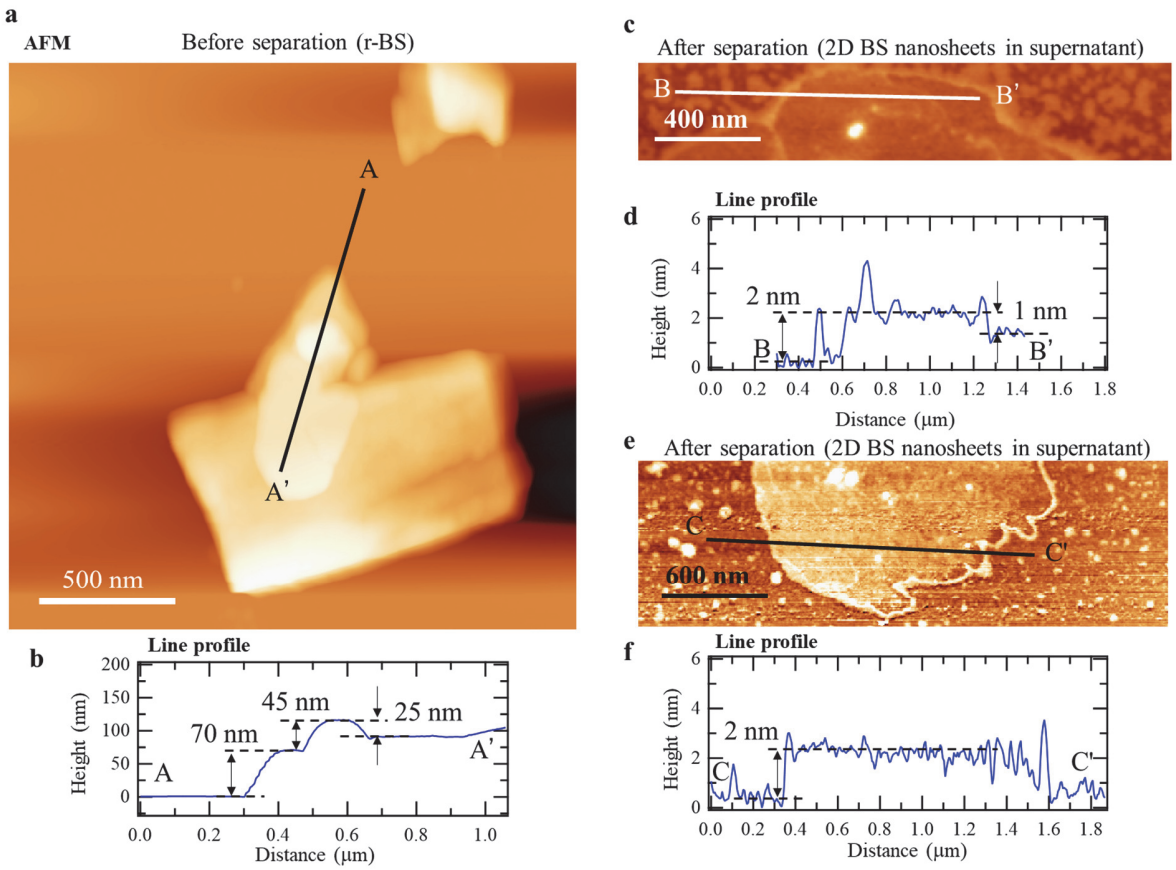

Figure S8. Atomic force microscopy (AFM) images of r-BS and 2D BS nanosheets. **a** AFM image of r-BS (before separation). **b** Profile along the line between points A and A' in panel a. **c** AFM image of 2D BS nanosheets (after separation). **d** Profile along the line between B and B' in panel c. **e** AFM image of 2D BS nanosheets (after separation). **f** Profile along the line between C and C' in panel e.

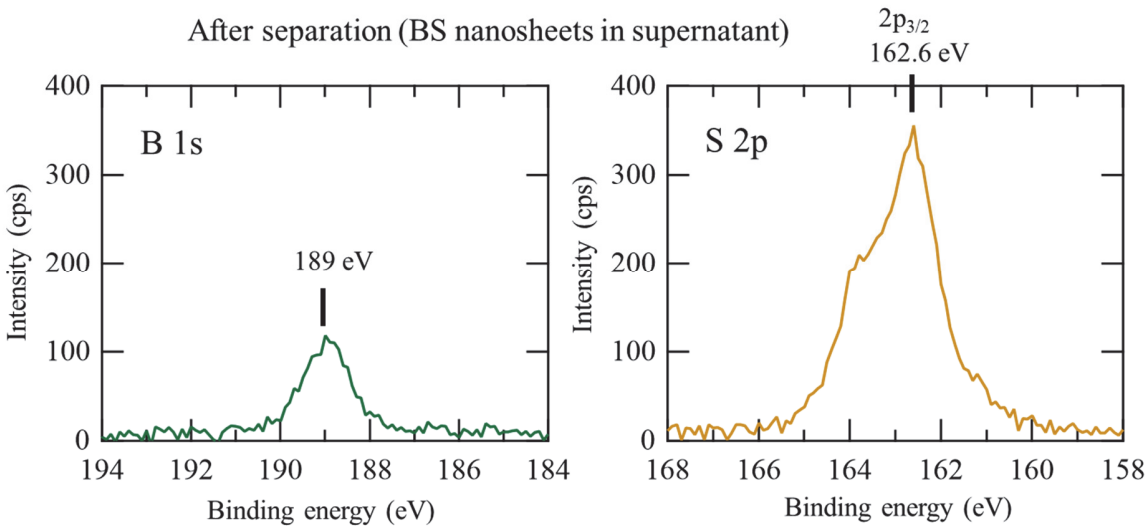

Figure S9. B 1s and S 2p X-ray photoelectron spectra of 2D BS nanosheets on an Au surface (after separation; i.e., removal of the solvent from acetonitrile supernatant by drying on the Au surface).

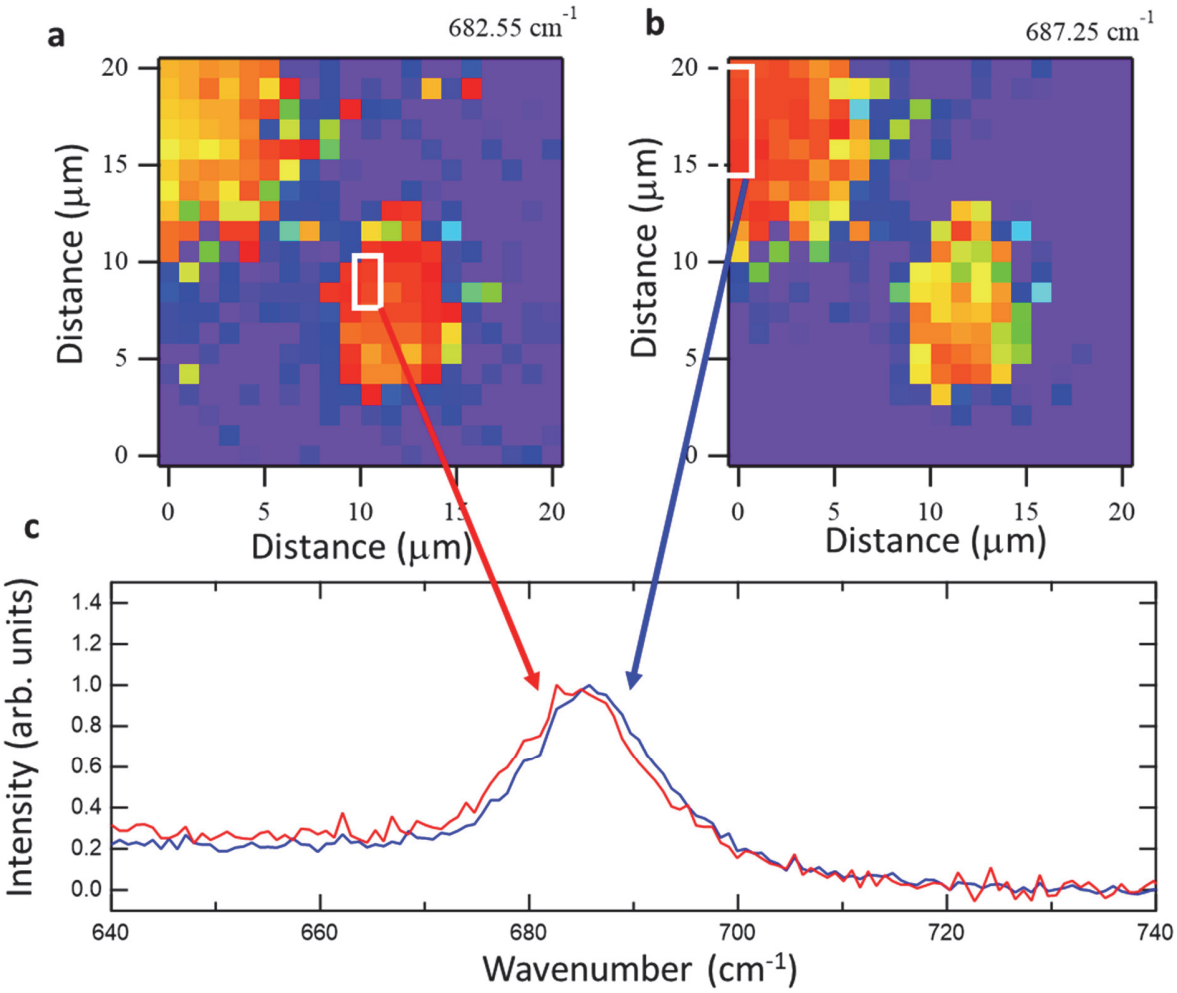

Figure S10. Raman mapping of as-synthesized r-BS powder on an Si surface. The intensity in each pixel was normalized against the maximum intensity in the range 670–700 cm^{-1}. **a.** Raman mapping at 682.55 cm^{-1}, where the intensity at 682.55 cm^{-1} was plotted as an image. **b.** Raman mapping at 687.25 cm^{-1}, where the intensity at 682.55 cm^{-1} was plotted as an image. **c**. Raman spectrum averaged at the indicated area in a (red curve) and b (blue curve), which shows a distinct difference between the peak position. According to the DFT calculation, the Raman peak position of the corresponding mode, E(4), is 709.29 cm^{-1} for one layer BS, 708.22 cm^{-1} for two-layer BS, 707.67 cm^{-1} for three-layer BS, and 705.29 cm^{-1} for bulk r-BS. Thus, there are 4 different wavenumbers between single layer BS and bulk r-BS, and the peak position depends on the thickness, as in the case of the bandgap. The experimental peak position difference indicates the presence of BS sheets with different thicknesses.

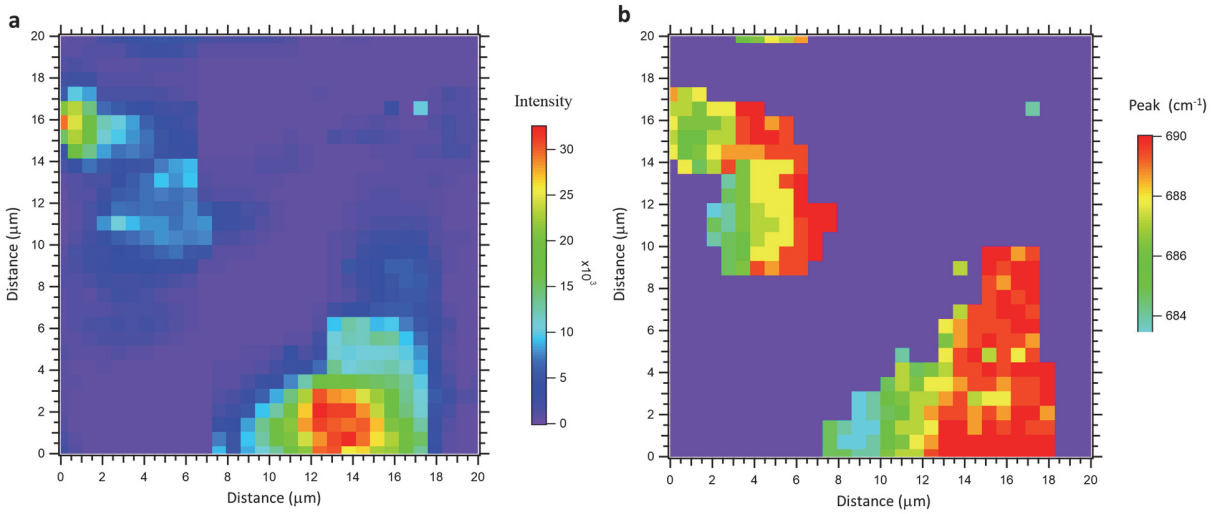

Figure S11. Raman mapping of the BS nanosheets on an Si surface. **a.** Raman intensity mapping, where the integral intensity from 670.48–701.95 cm^{-1} was plotted as an image. **b.** Raman peak mapping, where the intensity peak frequency in the range of 684–690 cm^{-1} was plotted as an image (after selecting the peak intensity above 3000 arb. units). Red color positions indicate thin nanosheets, while green color positions indicate thick nanosheets or bulk r-BS (see Figure S10).

References of Supplementary Information

1 D. A. Allison, G. Johansson, C. J. Allan, U. Gelius, H. Siegbahn, J. Allison and K. Siegbahn, *J. Electron Spectros. Relat. Phenomena*, 1972, **1**, 269–283.
2 W. L. J. D. N. Hendrickson, J. M. Hollander, *Inorg. Chem.*, 1970, **9**, 612–615.
3 K. D. Moulder, J.F.; Stickle, W.F.; Sobol, P.E.; and Bomben, *Handbook of X-Ray Photoelectron Spectroscopy.*, 1992.
4 J. S. Ozcomert and M. Trenary, *Chem. Mater.*, 1993, **5**, 1762–1771.
5 J. Zhu, C. He, Y. Li, S. Kang and P. K. Shen, *J. Mater. Chem. A*, 2013, **1**, 14700–14705.
6 J. Tai, J. Hu, Z. Chen and H. Lu, *RSC Adv.*, 2014, **4**, 61437–61443.
7 S. Perkins, C.L.; Trenary, M.; Tanaka, T.; Otani, *Surf. Sci.*, 1999, **423**, L222–L228.
8 C. G. Cermignani, W.; Paulson, Thomas E.; Onneby, C.; Pantano, *Carbon N. Y.*, 1995, **33**, 367–374.
9 M. Trenary, *Sci. Technol. Adv. Mater.*, 2012, **13**, 023002.
10 S. Patil, G. Adhikary, G. Balakrishnan and K. Maiti, *Solid State Commun.*, 2011, **151**, 326–328.
11 G. Mavel, J. Escard, P. Costa and J. Castaing, *Surf. Sci.*, 1973, **35**, 109–116.
12 M. Menetrier, T. Shirasaki, A. Derre, A. Tressaud and S. Flandrois, *Carbon N. Y.*, 2000, **38**, 1461–1467.
13 T. Aizawa, S. Suehara, S. Hishita, S. Otani and M. Arai, *Phys. Rev. B - Condens. Matter Mater. Phys.*, 2005, **71**, 1–9.
14 H. Nishino, T. Fujita, N. T. Cuong, S. Tominaka, M. Miyauchi, S. Iimura, A. Hirata, N. Umezawa, S. Okada, E. Nishibori, A. Fujino, T. Fujimori, S. Ito, J. Nakamura, H. Hosono and T. Kondo, *J. Am. Chem. Soc.*, 2017, **139**, 13761–13769.
15 L. Bao, X. Qi, Tana, L. Chao and O. Tegus, *CrystEngComm*, 2016, **18**, 1223–1229.
16 K. B. Garg, T. Chatterji, S. Dalela, M. Heinonnen, J. Leiro, B. Dalela and R. K. Singhal, *Solid State Commun.*, 2004, **131**, 343–347.
17 A.Talapatra, S. K. K. Bandyopadhyay, P. Sen, P. Barat, S. Mukherjee, M. Mukherjee, A. Talapatra, S. K. K. Bandyopadhyay, P. Sen, P. Barat, S. Mukherjee and M. Mukherjee, *Phys. C Supercond. its Appl.*, 2005, **419**, 141–147.
18 R. P. Vasquez, C. U. Jung, M. S. Park, H. J. Kim, J. Y. Kim and S. I. Lee, *Phys. Rev. B - Condens. Matter Mater. Phys.*, 2001, **64**, 0525101–0525104.
19 B. J. Lindberg, K. Hamrin, G. Johansson, U. Gelius, A. Fahlman, C. Nordling and K. Siegbahn, *Phys. Scr.*, 1970, **1**, 286–298.
20 R. S. C. Smart, W. M. Skinner and A. R. Gerson, *Surf. Interface Anal.*, 1999, **28**, 101–105.
21 M. Fantauzzi, A. Rigoldi, B. Elsener, D. Atzei and A. Rossi, *J. Electron Spectros. Relat. Phenomena*, 2014, **193**, 6–15.
22 J. Yuan, J. Wen, Y. Zhong, X. Li, Y. Fang, S. Zhang and W. Liu, *J. Mater. Chem. A*, 2015, **3**, 18244–18255.
23 G. Pagona, C. Bittencourt, R. Arenal and N. Tagmatarchis, *Chem. Commun.*, 2015, **51**, 12950–12953.
24 R. Morrish, R. Silverstein and C. A. Wolden, *J. Am. Chem. Soc.*, 2012, **134**, 17854–17857.
25 S. L. Yang, H. Bin Yao, M. R. Gao and S. H. Yu, *CrystEngComm*, 2009, **11**, 1383–1390.
26 L. Sangaletti and F. Parmigiani, *Phys. Rev. B - Condens. Matter Mater. Phys.*, 1997, **55**, 9514–9519.
27 Y. H. Chang, C. Te Lin, T. Y. Chen, C. L. Hsu, Y. H. Lee, W. Zhang, K. H. Wei and L. J. Li, *Adv. Mater.*, 2013, **25**, 756–760.
28 T. Weber, J. C. Muijsers, J. H. M. C. Van Wolput, C. P. J. Verhagen and J. W. Niemantsverdriet, *J. Phys. Chem.*, 1996, **100**, 14144–14150.
29 T. Fujita, Y. Ito, Y. Tan, H. Yamaguchi, D. Hojo, A. Hirata, D. Voiry, M. Chhowalla and M. Chen, *Nanoscale*, 2014, **6**, 12458–12462.
30 B. Jariwala, D. Voiry, A. Jindal, B. A. Chalke, R. Bapat, A. Thamizhavel, M. Chhowalla, M. Deshmukh and A. Bhattacharya, *Chem. Mater.*, 2016, **28**, 3352–3359.
31 X. Chia, A. Ambrosi, P. Lazar, Z. Sofer and M. Pumera, *J. Mater. Chem. A*, 2016, **4**, 14241–14253.
32 M. Fantauzzi, B. Elsener, D. Atzei, A. Rigoldi and A. Rossi, *RSC Adv.*, 2015, **5**, 75953–75963.
33 X. L. Qiu, X. H. Gao, T. H. Zhou, B. H. Chen, J. Z. Lu, H. X. Guo, X. T. Li and G. Liu, *Sol. Energy*, 2019, **181**, 88–94.
34 C. Pfohl, A. Bulak and K. T. Rie, *Surf. Coatings Technol.*, 2000, **131**, 141–146.
35 L. Shi, Y. Gu, L. Chen, Z. Yang, J. Ma and Y. Qian, *Inorg. Chem. Commun.*, 2004, **7**, 192–194.
36 K. Ueda, H. Yamamoto and M. Naito, *Phys. C Supercond. its Appl.*, 2002, **378–381**, 225–228.
37 D. Gonbeau, H. Bouih, G. Pfister-Guillouzo, M. Menetrier and A. Levasseur, *J. Chem. Soc. Faraday Trans.*, 1995, **91**, 93–97.
38 E. A. Il'Inchik, *J. Appl. Spectrosc.*, 2008, **75**, 883–891.